Sensor platform of the Hybrid E-Tattoo (May 2024)

Laurence Jorissen, student, UHasselt & KU Leuven
Thijs Vandenryt (imo-imomec) (supervisor)

***Abstract*—Wearable devices have emerged as life-changing tools in healthcare, and the Hybrid E-Tattoo aims to play a significant role in this field. It is a hybrid wearable plug-and-play healthcare device, that combines smart textiles and skin adhesives to read out multiple sensors. The readout of these sensors occurs at a centralized platform, known as the sensor platform. Using a combination of digital and analog sensors, standard wiring, and silver plated yarn, a demonstrator was created to showcase the feasibility of the sensor platform integrating these components. The demonstrator produced clear results, indicating that sensor fusion with smart textiles and skin adhesives is possible. However, further research is needed to optimize and refine the technology.**

***Index Terms*— electronics, healthcare, sensor fusion, wearable device, textile**

I. Introduction

In recent years, wearable devices have emerged as life-changing tools in healthcare, offering the promise of continuous monitoring and personalized telemedicine. Yet, their integration into everyday life presents unique design challenges and implications, particularly in ensuring usability by non-medical users across diverse environments. However, employing a small-scale wearable, that captures and displays sensed body data on visible screens, offers notable advantages. From monitoring biological signals, to tracking metabolic status, wearable medical devices offer not only the promise of a healthier lifestyle, but also invaluable data for disease diagnosis and treatment. As such, they stand to become essential in the future of mobile medicine, enhancing individuals' self-awareness concerning their health and contributing to the progress of healthcare practices [1], [2].

A. Hybrid E-Tattoo project

The Hybrid E-Tattoo project introduces a wearable sensor technology platform designed to revolutionize health monitoring from an electronic perspective. Unlike existing digital wearables that often rely on single sensors, this project aims to create a versatile hybrid plug-and-play platform capable of measuring various parameters such as temperature, oxygen saturation, and breathing rate, among others. As seen on figure 1, this innovation integrates smart textiles with on-skin patches (E-Tattoos), allowing for the fusion of different sensors to provide comprehensive insights into the wearer's well-being and health status [3], [4], [5].

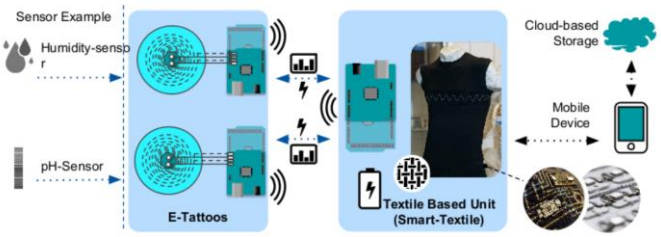

Figure 1: Summary of the Hybrid E-Tattoo project[4]

In the middle part of Figure 1, between the E-Tattoos and the textile-based unit (Smart-Textile), communication is necessary between all the different devices. This setup introduces a potential problem, as it could result in a tangled mess of wires. The solution is a centralized platform for all devices and sensors to connect to, known within this project as the "sensor platform".

B. The sensor platform of the Hybrid E-Tattoo

This platform serves as a crucial innovation, acting as a centralized hub for managing data from all sensors. It enables data collection, which can then be forwarded to other devices or stored in a database for further analysis. Different devices are interconnected to the platform using smart textiles, while a disposable bottom section, as shown in Figure 2, houses embedded resistance-based analog sensors, forming the core of the E-Tattoo. This integration significantly enhances the functionality of the wearable, marking a shift in wearable technology.

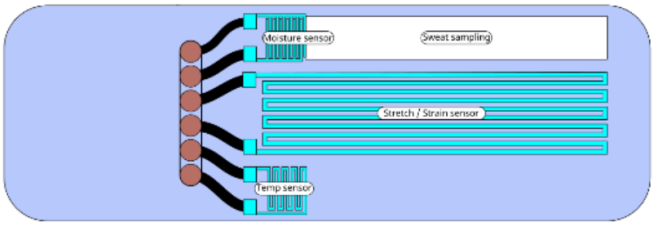

Figure 2: The disposable part of the Hybrid E-Tattoo, which is an electronic skin patch with integrated analog sensors, is located beneath the sensor platform.

The main focus will be on the development of the sensor platform itself. The primary goal is to demonstrate the capability to read data from various digital and analog sensors using standard wiring and silver plated yarn simultaneously. Silver plated yarn is highly conductive and antimicrobial, meaning it can be easily sewn into clothing to create electronic textiles which have to attain certain hygienic requirements [22].

Figure 3 showcases the blueprint of the sensor platform and all its different connection areas to the disposable part, the main microcontroller, off-the-shelf digital sensors and the magnetic interconnection.

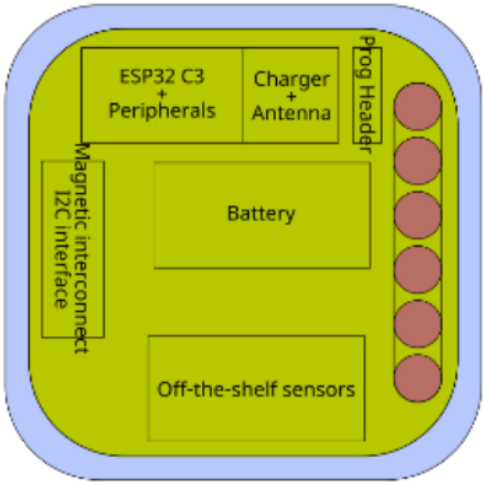

Figure 3: The blueprint of the sensor platform for the Hybrid E-Tattoo, including all its connections to various sensors and devices.

Since the different sensors are placed on various parts of the body, each cable, wire, or piece of silver yarn will have a unique length. As the cable length between the sensor platform and a sensor or device increases, both the capacitive load and the resistance of the cable will increase. This combination of increased resistance and capacitance can negatively affect the communication protocol between the microcontrollers and digital sensors. The increased resistance can lower the peak voltage of the square wave, while the increased capacitance can distort the signal and introduce errors [6], [7]. As shown in the figure below, the well-formed signal provides a clear distinction between a 0 and a 1 to the microcontroller. However, as the cable length increases, the signal becomes significantly distorted, making it more difficult for the microcontroller to accurately recognize the difference between a 0 and a 1. Keeping this occurrence of signal distortion in mind before building the sensor platform would be of great advantage.

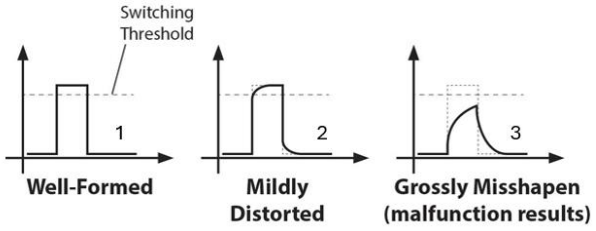

Figure 4: Test pulses distorted by output impedance and natural cable capacitance (pulses 1 & 2), can lead to malfunction (pulse 3) [6]

II. Materials and Methods

Firstly, the core of the sensor platform is the microcontroller mounted on a custom Printed Circuit Board (PCB) with various connections and components. For this project, the microcontroller used is the Wemos C3 Pico V1.0.0 - Lolin WiFi IoT board ESP32-C3. It can handle the readout of each sensor and transmit all the information to an online database. The code for this microcontroller was written in C++ using an Integrated Development Environment (IDE) called PlatformIO. InfluxDB is the database used to store the collected data. The code written on the microcontroller includes sensor implementations, settings, and readouts. It features a function that identifies each digital sensor connected to the multiplexer and an average sampling function that calculates the average value for each analog temperature sensor. Additionally, the code handles the connection and data transmission to InfluxDB [8].

To read out all the digital sensors, each sensor must be connected to the 3.3 volts, ground, serial clock line, and serial data line of the microcontroller. The I2C protocol, a synchronous multi-controller serial communication bus, is designed for short-distance communication between integrated circuits and microcontrollers [9]. In this project, the cable length will be increased while maintaining the same signal quality.

In the setup, the microcontroller on the sensor platform serves as the master, while another microcontroller, along with all the sensors, functions as a slave. Each sensor type and microcontroller will possess its unique 7-bit address. A microcontroller can communicate with various sensors and other microcontrollers, provided each device on the I2C bus has a unique device address. This implies that a slave cannot transmit data unless it has been addressed by the master [10], [11]. Therefore, the TCA9548A 1-to-8 I2C multiplexer were employed to facilitate communication with sensors and devices sharing the same 7-bit address. The digital sensors and multiplexer used are listed below:

- The BH1750 is a digital light sensor that measures light intensity in lux [12].
- The BMP280 sensor is an environmental sensor measuring temperature, barometric pressure, and altitude [13].
- The MAX30102 or the PPG (photoplethysmography) sensor is an oximeter and heart rate sensor [14].

The TCA9548A 1-to-8 I2C multiplexer enables connecting up to 8 devices with the same I2C address to a single microcontroller. Acting as a gatekeeper, it directs commands to the selected set of I2C pins based on input instructions. The multiplexer itself can have addresses ranging from 0x70 to 0x77, allowing for the possibility of connecting up to 64 sensors of the same type with the same address [15].

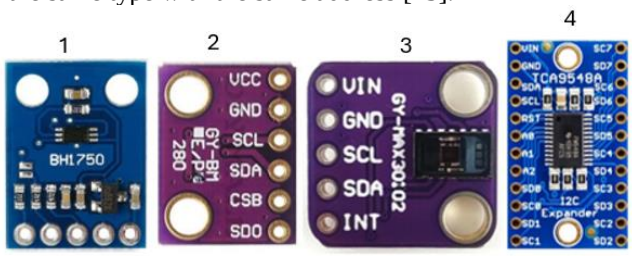

Figure 5: The light (1), humidity (2) and PPG sensor (3) and the multiplexer (4)

To address the issue of capacitive load, a separate device is required to restore the original square wave of the signal by adding current. The LTC4311 is a dual I2C active pull-up designed to enhance data transmission speed and reliability under bus loading conditions that exceed the I2C specification

limit [16]. This device monitors the SDA and SCL lines and, when the signal becomes distorted, it provides the additional current needed to restore the original square wave [17].

Figure 6: The LTC 4311

For the analog sensors seen in Figure 7, screen-printed temperature sensors made from silver paste containing silver nanoparticles were used. Resistance measurements serve as a temperature readout, since resistance increases with temperature [18].

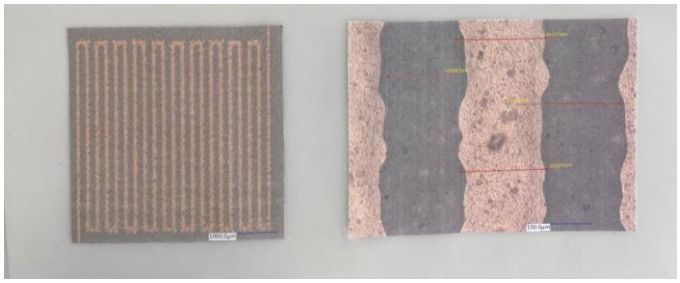

Figure 7: The screen printed analog temperature sensor

In the microcontroller's program, the resistance calculations are performed using the following formula of a voltage divider:

$$V_{out} = \frac{R_{temp}}{R_{pre-connected} + R_{temp}} * V_{in} \qquad (1)$$

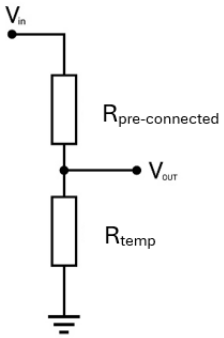

Figure 8: Voltage divider circuit

Each sensor needs to be connected to an analog pin and the ground pin of the microcontroller. While the pre-connected resistance is known, *V*out will be obtained by the microcontroller using the "readVoltage()" function. The ADC (Analog-to-Digital Conversion) inside the microcontroller is used to convert the analog voltage into a digital value. ADC attenuation allows for adjusting the maximum measurable voltage for the microcontroller, thereby improving the precision of the measurement. The range of measured voltage spans from 0 to *V*ref . There are four available attenuation options (Table 1) whereby higher attenuation allows for a higher measurable input voltage [19].

TABLE I
ATTENUATION OPTIONS

Attenuation	Measurable input voltage range
ADC_ATTEN_DB_0	0 mV – 750 mV
ADC_ATTEN_DB_2_5	0 mV – 1050 mV
ADC_ATTEN_DB_6	0 mV – 1750 mV
ADC_ATTEN_DB_11	0 mV – 2500 mV

The voltage based on attenuation change can be calculated with the following formula:

$$V_{out} = D_{out} * (\frac{V_{max}}{D_{max}}) \qquad (2)$$

Where Vout is the digital output voltage of the microcontroller, Dout is the ADC raw digital reading result. Vmax is the maximum measurable input voltage from the ADC attenuation. And Dmax is the maximum of the output ADC raw digital reading result, which is 4095 bytes [19]. After the calculations of Vout, Rpre-connected can be calculated.

Furthermore, the microcontroller's program includes an averaging method to obtain more consistent results. The method functions as follows: each measured resistance is stored in an array of a chosen length. Initially, any empty spaces in the array, where no measurement has been placed, are filled with zeros. Consequently, the average resistance calculation is of significance only after the array is fully populated. With each new measurement, the oldest measurement at the beginning of the array is replaced by the newest one. Simultaneously, all measurements are summed up and subsequently divided by the length of the array to obtain an averaged result of the analog temperature sensors.

Silver yarn was employed for communication between the two microcontrollers, using I2C communication with one acting as the master and the other as the slave. To compensate for the higher resistance of the silver yarn compared to a standard flat cable [23], the voltage was increased to 12V to ensure an adequate current supply to power the slave microcontroller. Consequently, a LM2577 Step-Up Voltage Regulator was used at the master microcontroller to boost the voltage, while a DC-DC step-down buck converter, such as the MP2307, was employed at the slave microcontroller to lower the voltage.

To ensure security and minimize signal noise, additional components such as resistors, capacitors, ESD suppressors, ferrite beads, a 0.5 milliAmps fuse, and a MOSFET P-ch -30 Volts 13.5 Ampere transistor were incorporated into the design. Resistors served as pull-up resistors for I2C communication, with some being sourced from the multiplexer device itself and placed onto the PCB. Ferrite beads and ESD suppressors were employed to facilitate long-distance communication for certain

sensors. The transistor and fuse provide reversed polarity protection.

For the sensor platform, a 2-layer PCB where all components come together was designed using KiCad. There were no specific requirements that needed to be met. To obtain data, either a program called Serial Studio, which allows for easy collection of data from each sensor into the same file, or an oscilloscope was used [20].Simulation of the sensor platform with all devices and sensors connected was realized with a demonstrator. This demonstrator consisted of a plastic plate where all devices were assigned their own area, connected on the outside, with silver yarn spread across the middle of the plate to enable communication from one side to the other.

III. Results

A. *The sensor platform*

Figure 9 and 10 depict a 2D view of the front and back side of the developed sensor platform, created in KiCad. The drawing illustrates all the various components and connections to sensors and devices.

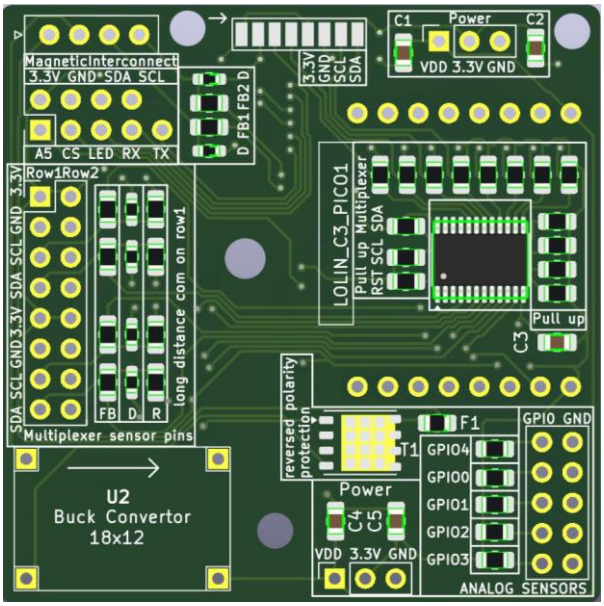

Figure 9: Front side of the sensor platform drawing

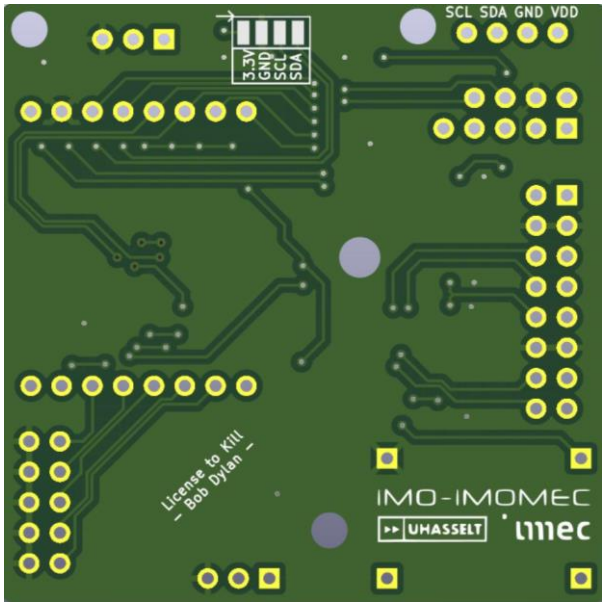

Figure 10: Back side of the sensor platform drawing

B. *The demonstrator*

The constructed demonstrator seen in Figure 11, comprises various components for data sensing and readout, interconnected via both conventional wires and textiles (silver plated yarn). On number 1 in the figure there is the sensor platform, number 2 contains the analog temperature sensors, number 3 is the boost convertor, number 4 are the different digital sensors and the multiplexer, number 5 is the buck convertor and the second microcontroller that acts as a slave and sends its data back to the sensor platform.

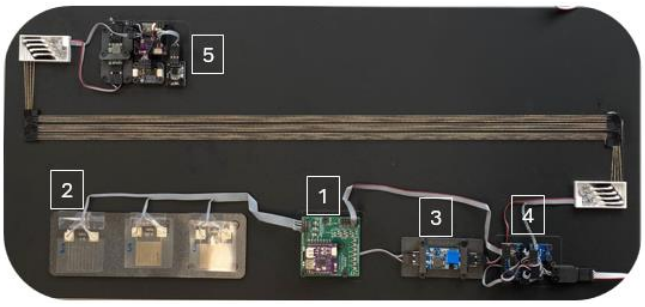

Figure 11: The demonstrator showcasing all the different sensors and devices

C. *Analog temperature sensors data*

The three figures below depict the data collected from the three analog temperature sensors. The sensors were heated from 0 to 180 seconds and then cooled down from 180 seconds to 400. Each sensor is connected to a pre-connected resistor with a value of 220 Ω. For the first sensor, the average resistance at room temperature was approximately 121 Ω, with a voltage value of 1.171 V. The second sensor had an average resistance of around 44.5 Ω at room temperature, corresponding to a voltage value of 0.555 V. For the third sensor, an average resistance of 14.4 Ω was measured at room temperature, with a voltage value of 0.203 V.

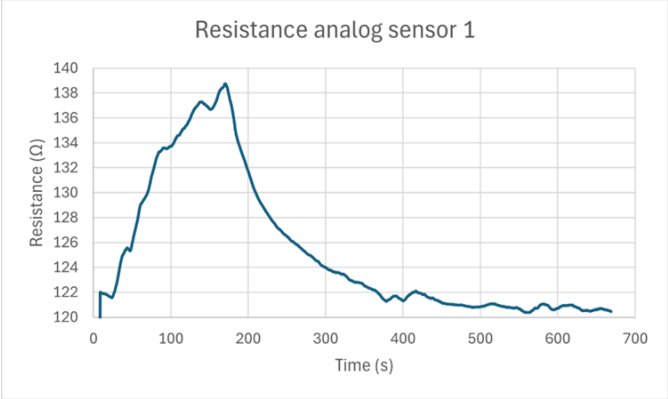

Figure 12: The resistance over time of the first analog temperature sensor when heated and cooled down

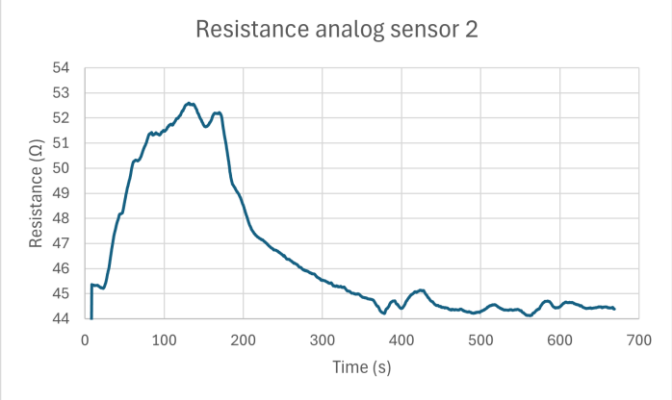

Figure 13: The resistance over time of the second analog temperature sensor when heated and cooled down

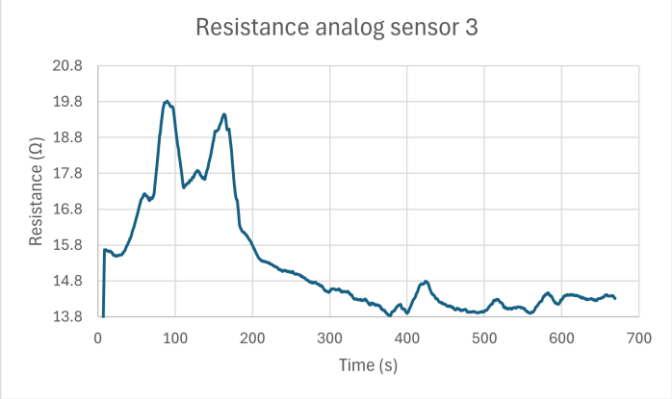

Figure 14: The resistance over time of the third analog temperature sensor when heated and cooled down

D. Off-the-shelf digital sensors data

For each following digital sensor there is a figure to show that they could all send data in the same testing cycle.

- The data collected from the PPG sensor. The PPG sensor measures 2 parameters, infrared (IR) light and red light (RED) (Figures 15 & 16)
- The room temperature measured from the BMP 280 humidity sensor (Figure 17).
- The atmospheric pressure measured from the BMP 280 humidity sensor (Figure 18).
- The altitude measured from the BMP 280 humidity sensor (Figure 19).
- The intensity of light measured from the BH 1750 light sensor (Figure 20).
- The I2C clock and data line seen from the oscilloscope without the use of the LTC 4311 (Figures 21 & 22).
- The I2C clock and data line seen from the oscilloscope with the use of the LTC 4311 (Figures 23 & 24).

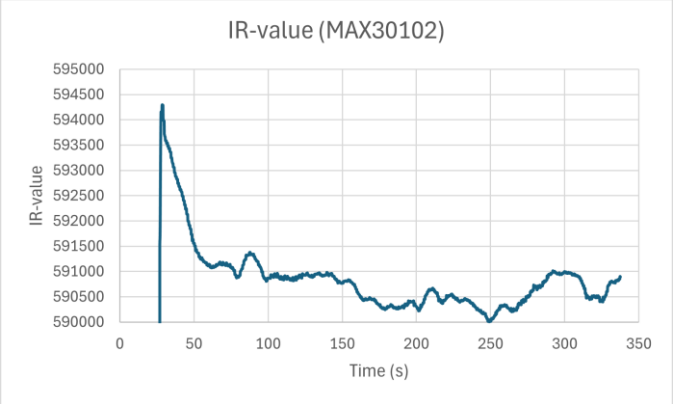

Figure 15: IR-Value data collected from the PPG sensor

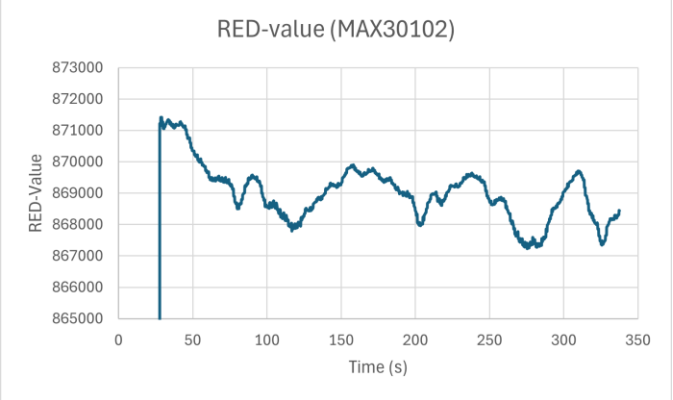

Figure 16: RED-Value data collected from the PPG sensor

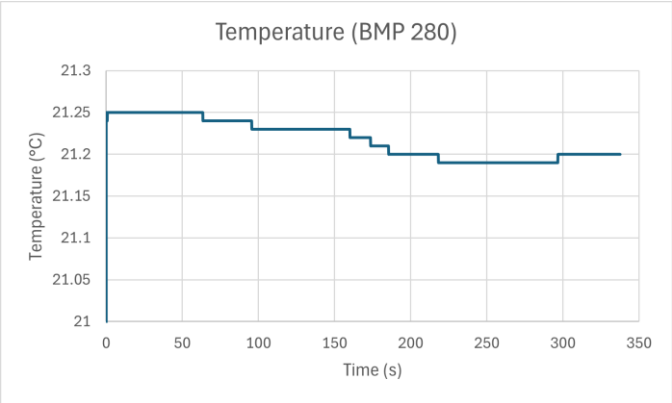

Figure 17: Temperature over time measured with the BMP 280 humidity sensor

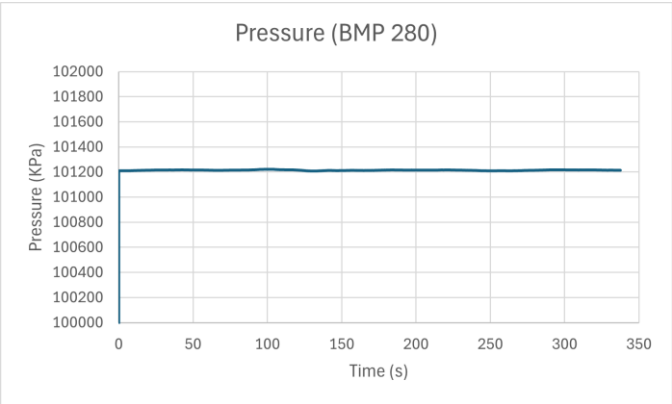

Figure 18:Atmospheric pressure measured over time from the BMP 280 humidity sensor

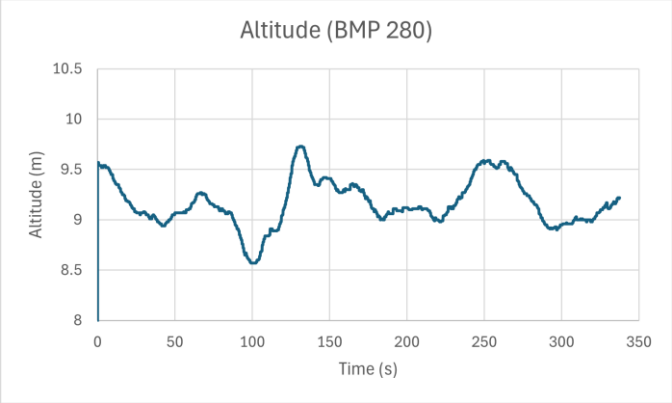

Figure 19: Altitude measured over time from the BMP 280 humidity sensor

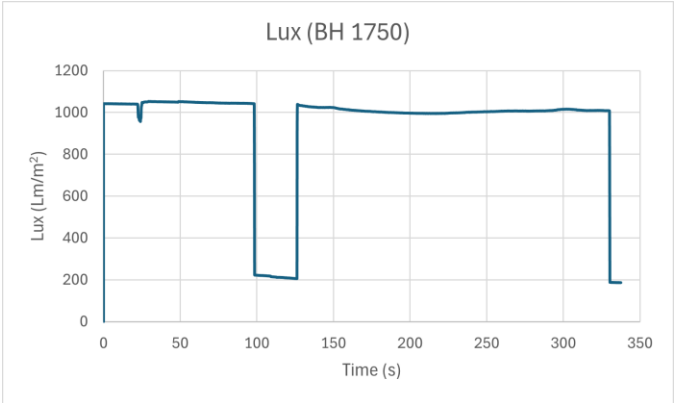

Figure 20: Lux measured over time from the BH 1750 light sensor

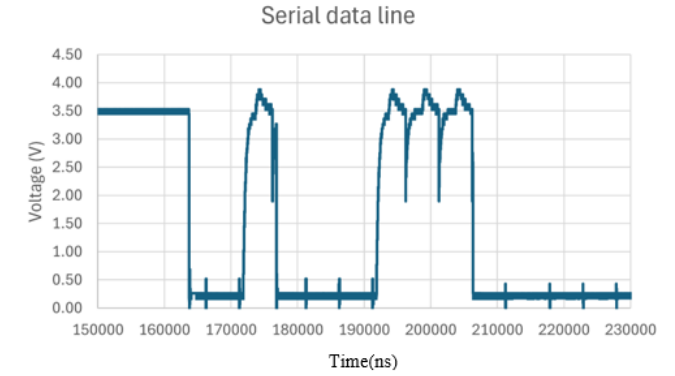

Figure 21: Serial data line from light sensor over standard wiring without LTC 4311

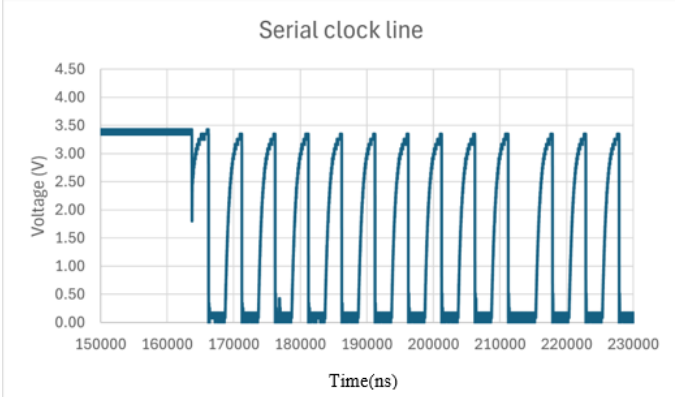

Figure 22: Serial clock line from light sensor over standard wiring without LTC 4311

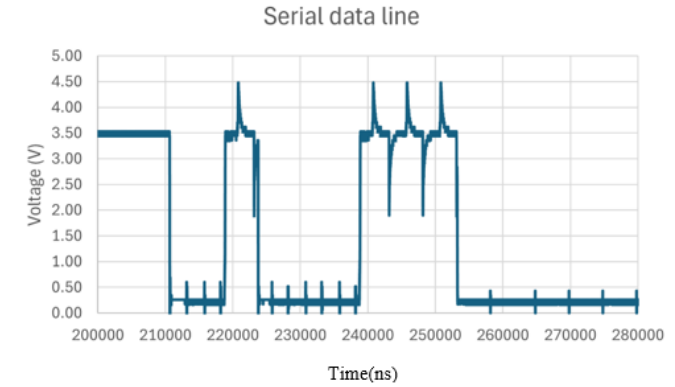

Figure 23: Serial data line from light sensor over standard wiring with LTC 4311

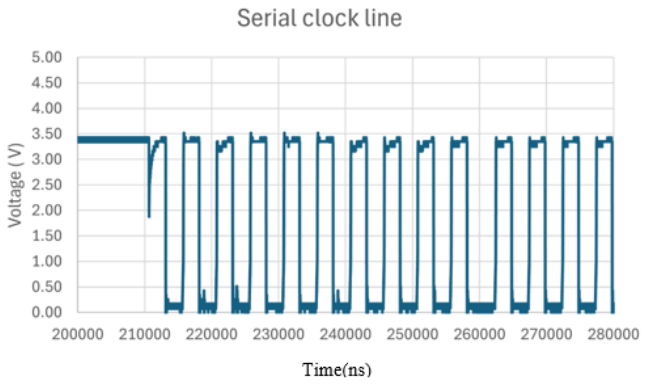

Figure 24: Serial data line from light sensor over standard wiring with LTC 4311

The next figures show a screenshot of the I2C communication between the master microcontroller and slave microcontroller with silver yarn.

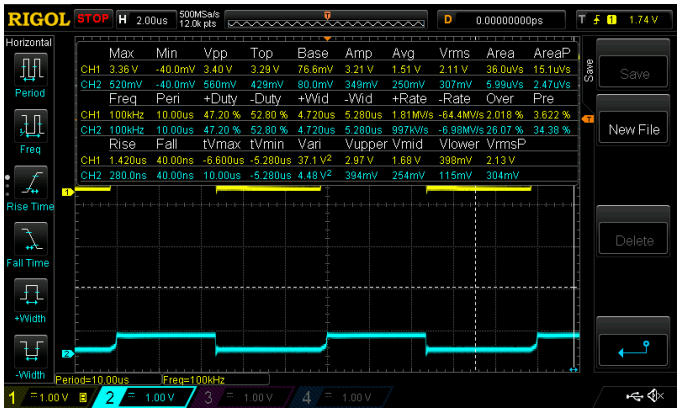

Figure 25: Serial clock line at the end of the silver yarn where the ground is connected through normal wiring

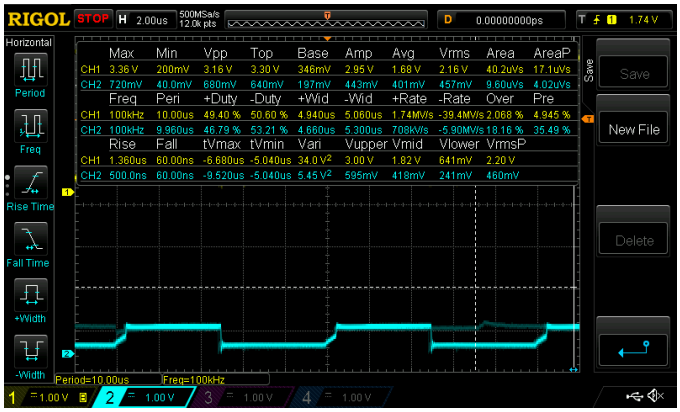

Figure 26: Serial clock line throughout only silver yarn

Figure 25 shows the clock data line at the end of the silver yarn where the ground is connected through normal wiring. The top of the square wave is 429 mV at the end of the silver yarn and 3.29V at the beginning of the silver yarn. Figure 26 shows the clock data line throughout the silver yarn using only the silver yarn. The top of the square wave is 640 mV at the end of the silver yarn and 3.30V at the beginning of the silver yarn.

IV. Discussion

The demonstrator showcased that the communication and the readout of all the sensors worked throughout standard wiring or silver yarn.

From the results of all the digital sensors, it can be concluded that the readout of each sensor performs correctly. As seen in the graphs from Figures 15 to 20, there are no errors when reading data from the sensors, using the I2C communication protocol with a standard flat cable, approximately 2 meters in length. The goal was to determine whether it is possible to obtain data from these sensors over a longer distance, with the expectation that errors might occur due to the increased distance. However, no errors were found for short and long wires, likely due to the low resistance of the wires used. The signal, as shown in the graphs, provides a pulse with a full range up to 3.3 Volts.

For the readout of the digital sensors using silver yarn, the top of the pulse decreases significantly, as seen in Figure 25. This is due to the silver yarn having a much higher resistance than the normal flat cable wire. Whereas a normal flat cable wire has a resistance of approximately 8 ohms over 2 meters, the silver yarn has a resistance of approximately 108 ohms over 1.5 meters. The increased resistance lowers the maximum voltage as it decreases the maximum current allowed to the sensor [21]. This was not a problem for the readout of the digital sensor, but it was for the communication with the slave microcontroller.

With the use of the LM2577 Step-Up Voltage Regulator and an MP2307 buck converter, it was possible to power the slave microcontroller and read data from the sensor, but when sending its data back to the master microcontroller on the sensor platform through the silver yarn, a problem occurred.

As seen in Figure 25, on Channel 2 of the microcontroller, there is a small, clean block wave representing the address that the slave microcontroller sends to the master microcontroller through the silver yarn, with the ground wired using standard flat cable wire. In Figure 26, Channel 2 represents the same signal, except the ground is connected with silver yarn. Comparing Figure 26 with Figure 25, it is evident that on Channel 2 there is a small stretch on the rising edge of the block wave, and the base of the block wave is increased for both Channel 1 and Channel 2.

This occurrence could be due to various factors. Such as bad wiring or poor connections. There is also a possibility that the slave microcontroller isn't able to send enough current back through the silver yarn. However, further research is needed to determine the exact cause.

Even without the LTC 4311 component the signal is still clear enough as seen on figures 21 to 24, the microcontroller can still differentiate between a 0 and a 1 in the I2C communication protocol. This means that the current use of the LTC 4311 is unnecessary. The LTC 4311 would only be useful if the capacitive load of the wire becomes too high. In such a

scenario, this component would apply current to restore the original block wave, as seen when comparing Figures 22 and 24. Nonetheless, it serves as a demonstration to show that there is a solution available if the capacitive load becomes too high.

The readout of the analog sensors also worked as expected. The goal was to first measure the resistance at room temperature with the microcontroller, using the voltage divider formula (1), and observe an increase in resistance as the sensors were heated, and a decrease in resistance as the sensors cooled down. As shown on figures 12 to 14, this goal was attained. However, there is significant room for optimization. Each temperature sensor was paired with a pre-connected resistor valued at 220 Ω, to demonstrate their functionality. As seen in Figure 12, the first sensor had the best resolution, since the same ADC attenuation, at 6dB, was used for each sensor, corresponding to a voltage range of 0–1750 mV. The voltage value at room temperature of the first sensor matched best within this range, whereas the other sensors had much lower voltage values. Each of the 3 figures represents a different resistance value at room temperature due to the varying width and length of the path on the sensor itself, seen on Figure 7. The thinner and longer the paths, the higher the resistance of the sensor [18]. Therefore, the path in the first graph is the thinnest and longest of the three sensors. The difference in resolution among the three sensors is likely due to this setup. To increase the resolution, one could modify the attenuation for each sensor individually or use a pre-connected resistor with a fixed value for each sensor, which places the temperature sensor in a voltage range of 0-1750 mV.

Finally, it's important to note that the sensor platform PCB seen in Figures 9 and 10 is not the same prototype as the one used on the demonstrator seen in Figure 11. However, the functionality of the different prototypes remained the same. The design in Figures 9 and 10 is a more optimized version, with the addition of the multiplexer chip, buck converter, and all components necessary for security and long-distance communication. Regarding the drawing of the sensor platform itself, there weren't any strict rules or significant issues to consider. All the pins and components simply needed their own space, and the PCB accommodated every connection. There is still a lot of room for improvement in designing the layout of the sensor platform. Design optimization would be more about personal preferences rather than the requirements of the project itself.

V. Conclusion

To conclude this project, it is safe to say that the current demonstrator of the sensor platform demonstrates great potential within the Hybrid E-Tattoo project. However, to obtain a fully functional product, significant optimalization is still required in all aspects of the project. For instance, there is room for improvement with the digital sensors, particularly in the calibration process. Similarly, optimization opportunities exist for the analog sensors, such as enhancing resolution and potentially integrating external amplifiers for improved readout. Once calibration and resolution issues are addressed, optimization of the dataflow to the database can be enhanced to ensure efficient data compression. Furthermore, it's worth noting that the sensor platform design primarily prioritized electronic aspects over healthcare considerations. In the future, as the sensor readouts consist of meaningful data, the original design can be adapted to better accommodate specific user cases and healthcare needs.

Acknowledgment

I would like to express my gratitude to my supervisor, Ing. Thijs Vandenryt, for his continuous support, guidance, and invaluable insights throughout the course of this project. His expertise and encouragement have been instrumental in the successful completion of this work.

I am also thankful to Juul Goossens and Lambert Jorissen for their collaborative efforts, constructive feedback, and technical assistance during this project.

At last, I would like to thank Professor Wim Deferme and Professor Ronald Thoelen for their support and valuable input throughout this project.

References

[1] C. Glaros and D. I. Fotiadis, "Wearable devices in healthcare," in Studies in fuzziness and soft computing, 2005, pp. 237–264.

[2] A. Anzanpour et al., "Self-awareness in remote health monitoring systems using wearable electronics," Design, Automation & Test in Europe Conference & Exhibition (DATE), 2017, Lausanne, Switzerland, 2017, pp. 1056-1061.

[3] "Hybrid E-Tattoo - Hochschule Kaiserslautern," Hochschule Kaiserslautern. https://www.hs-kl.de/hochschule/aktuelles/menschen-und-projekte/hybrid-e-tattoo

[4] T. Gries, T. Lauwigi, and R. Oberlé, "Projekttitel: Hybrid E-Tattoo -Eine Plattform für die Sensorfu- sion von intelligenten Textilien und Hautklebern für die nächste Generation von intelligenten Wearab- les." February 13, 2023. [Online]. Available: https://www.ita.rwth-aachen.de/global/show_document.asp?id=aaaaaaaabwxucoe [Accessed: May 16, 2024].

[5] "detail- UHasselt- UHasselt," *UHasselt*. https://www.uhasselt.be/en/projects/detail/24097-project-r-13197

[6] C. Research, "Testing long cables," *CAMI Research*, Feb. 28, 2017. https://www.camiresearch.com/Campaigns/Web-Articles/electrically-testing-long-cables.html#:~:text=Capacitance%20increases%20with%20cable%20length,a%20shield%20around%20the%20conductors.&text=Good%2Dquality%20twisted%20pair%20Ethernet,about%2017%20pF%20per%20ft.

[7] Vedantu, "Relation between resistance and length," *VEDANTU*. https://www.vedantu.com/physics/relation-between-resistance-and-length

[8] UHasselt-Imo-Imomec, "Hybrid_E-Tattoo-Hub/ESP32_C3/src/main.cpp at main · UHasselt-imo-imomec/Hybrid_E-Tattoo-Hub," *GitHub*. https://github.com/UHasselt-imo-imomec/Hybrid_E-Tattoo-Hub/blob/main/ESP32_C3/src/main.cpp

[9] Wikipedia contributors, "I2C," *Wikipedia*, May 16, 2024. https://en.wikipedia.org/wiki/I%C2%B2C

[10] J. Valdez, J. Becker, and Texas Instruments Incorporated, "Understanding the I2C bus," report, 2015. [Online]. Available: https://www.ti.com/lit/an/slva704/slva704.pdf?ts=1716310667710&ref_url=https%253A%252F%252Fwww.google.com%252F#:~:text=A%20slave%20may%20not%20transmit,on%20the%20same%20I2C%20bus.

[11] Würth Elektronik eiSos GmbH & Co. KG, *Using multiple sensors on single I2C Bus*. 2023, pp. 1–13. [Online]. Available: https://www.we-online.com/catalog/media/o702307v410%20ANM005_Using_multiple_sensors_on_single_I2C_bus.pdf

[12] HobbyElectronica, "BH1750 digitale licht sensor - HobbyElectronica," *HobbyElectronica*. https://www.hobbyelectronica.nl/product/bh1750-digitale-licht-sensor/

[13] Otronic voor al uw Microcontrollers, Sensoren en Componenten, "Digitale Barometer druk Sensor Module BMP280," *OTRONIC*. https://www.otronic.nl/nl/digitale-barometer-druk-sensor-module-bmp280.html

[14] RobotShop Europe, “MAX30102 Oximeter en Hartslagsensormodule,” *RobotShop Europe*. https://eu.robotshop.com/nl/products/max30102-oximeter-and-heart-rate-sensor-module
[15] A. Industries, “TCA9548A I2C Multiplexer.” https://www.adafruit.com/product/2717
[16] Linear Technology Corporation, “LTC4311.” [Online]. Available: https://www.analog.com/media/en/technical-documentation/data-sheets/4311fa.pdf
[17] “AdaFruit LTC4311 I2C Extender / Active Terminator,” *Adafruit Learning System*, Oct. 07, 2020. https://learn.adafruit.com/adafruit-ltc4311-i2c-extender-active-terminator/overview
[18] M. Jose, G. Oudebrouckx, S. Bormans, P. Veske, R. Thoelen, and W. Deferme, “Monitoring body fluids in textiles: combining impedance and thermal principles in a printed, wearable, and washable sensor,” *ACS Sensors*, vol. 6, no. 3, pp. 896–907, Jan. 2021.
[19] “Analog to Digital Converter (ADC) - ESP32-C3 - — ESP-IDF Programming Guide v4.4 documentation.” https://docs.espressif.com/projects/esp-idf/en/v4.4/esp32c3/api-reference/peripherals/adc.html#adc-attenuation
[20] “Serial Studio - A dashboard for your embedded projects.” https://serial-studio.github.io/
[21] “What is Resistance? | Hioki.” https://www.hioki.com/us-en/learning/electricity/resistance.html#:~:text=When%20an%20electron%20differential%20exists,resistance%2C%20the%20greater%20the%20current.
[22] “Silver plated conductive yarn,” Baoding Texcraf New Material Technology Co., Ltd., May 20, 2022. [Online]. Available: https://www.texcraf-protection.com/Functional-yarn/Silver-plated-conductive-yarn.html#:~:text=Clothing%3A%20Silver%20plated%20yarns%20can,to%20enhance%20durability%20and%20conductivity.
[23] J. Mersch, H. Winger, Ercan Altinsoy, and C. Cherif, “Electromechanical Properties of Silver-Plated Yarns and Their Relation to Yarn Construction Parameters,” *Polymers*, vol. 15, no. 21, pp. 4210–4210, Oct. 2023.